

# Optical Measurement of Toxic Gases Produced during Firefighting Using Halons

KEVIN L. McNESBY,\* ROBERT G. DANIEL, ANDRZEJ W. MIZIOLEK, and STEVEN H. MODIANO

U.S. Army Research Laboratory, Aberdeen Proving Ground, Maryland 21005-5066 (K.L.M., R.G.D., A.W.M.); and Aberdeen Test Center, Aberdeen Proving Ground, Maryland 21005-5059 (S.H.M.)

Several optical techniques (FT-IR emission and absorption spectroscopy, mid- and near-infrared tunable diode laser absorption spectroscopy) have been used to measure toxic gases produced during inhibition of flames by halogenated hydrocarbons (Halons). Fire types studied include low-pressure premixed flames, counterflow diffusion atmospheric-pressure flames, open-air JP-8 (turbine fuel) fires, and confined JP-8 fires. Spectra are presented and analyzed for these fires inhibited by CF<sub>3</sub>Br (Halon 1301) and C<sub>3</sub>F<sub>7</sub>H (FM-200). For low-pressure premixed flames, spectra are presented which show production of the CF<sub>3</sub> radical in methane/oxygen/Ar flames inhibited by CF<sub>3</sub>Br. For large-scale fire testing, it is shown that the type and amount of toxic gases produced during fire inhibition are highly dependent on fire conditions and temperatures and that some species not considered important (CF<sub>2</sub>O) are often produced in significant amounts. Finally, it is shown that HF production, during inhibition of vehicle fires using FM-200, is highly dependent on time to suppression.

Index Headings: Halon; Flame inhibition; Toxic gas production; HF; CF<sub>2</sub>O.

## INTRODUCTION

The investigations at the Army Research Laboratory (ARL) into halogenated hydrocarbon (Halon) inhibition of flames began several years ago as a project† to elucidate mechanisms of suppression using low-pressure premixed flames. This investigation was expanded to include atmospheric-pressure counterflow diffusion flames and was further expanded by an ongoing collaboration with the Aberdeen Test Center (ATC) to evaluate new test methods and equipment for suppression of real fires occurring within the crew compartment of combat vehicles. Results of these studies have recently appeared in the literature.<sup>1,2</sup> Since beginning these investigations, we have also been measuring production of toxic gases during Halon inhibition of flames.

The purpose of this paper is to describe how the fire-inhibitant testing methodology in our lab changed as our focus expanded from controlled laboratory-scale fires to large-scale real fires. We also present some recent results, using laser-based diagnostics, of measurements of toxic gas production, and measurements of precursors to toxic gases, during Halon inhibition of laboratory-scale fires and real fires in ordinary and demanding environments. To our knowledge, this is the first report of optical measurement of the CF<sub>3</sub> radical in inhibited, premixed, low-

pressure flames and is the first report of quantitative, *in situ*, real-time measurements of HF gas production during large-scale fire fighting by Halons.

The fire types investigated for production of toxic gases during inhibition by Halons range from laboratory-scale controlled flames to air-fed turbine fuel (JP-8) pan fires. Laboratory controlled flames include low-pressure premixed CH<sub>4</sub>/O<sub>2</sub>/Ar and CH<sub>4</sub>/air flames and atmospheric-pressure CH<sub>4</sub>/O<sub>2</sub> and CH<sub>4</sub>/air counterflow diffusion flames.<sup>1,2</sup> Real fires include open-air JP-8 pan fires<sup>3</sup> and confined JP-8 pan fires. Gas production was measured by using optical diagnostics including mid-infrared tunable diode lasers (MIR-TDLs), near-infrared tunable diode lasers (NIR-TDLs), and Fourier transform infrared (FT-IR) absorption and emission spectroscopy. Inhibitors investigated include CF<sub>3</sub>Br (Halon 1301), C<sub>3</sub>F<sub>7</sub>H (FM-200), C<sub>3</sub>F<sub>6</sub>H<sub>2</sub> (FE-36), C<sub>2</sub>F<sub>5</sub>H (FE-25), CF<sub>3</sub>H (FE-13), and CF<sub>4</sub>. For this report, inhibition only by CF<sub>3</sub>Br (Halon 1301) and C<sub>3</sub>F<sub>7</sub>H (FM-200) will be discussed.

## EXPERIMENTAL

Details of the experimental apparatus and equipment used in some of these measurements have been previously published<sup>1-3</sup> but will be summarized in what follows.

**Laboratory-Scale Fires. Low-Pressure Premixed Flames.** The experimental apparatus consists of a low-pressure flat flame burner (McKenna Industries, Inc.) mounted on translational stages inside an evacuable chamber. The evacuable chamber is equipped with apertured LiF windows (1.5 mm diameter) to allow passage of infrared laser radiation. Since the infrared laser beam or modulated FT-IR beam used to probe the burner flame remains fixed in position relative to the low-pressure burner chamber, different parts of the flame are examined by moving the burner within the chamber. Typical gas flow rates were 0.95 L/min CH<sub>4</sub>, 1.9 L/min O<sub>2</sub>, and 3.0 L/min Ar. Argon was used as a diluent in order to lower the peak flame temperature to the working range of Pt-Pt/Rh thermocouples (~2000 K). Inhibitant flow was typically less than 2% of the total (fuel plus oxidizer) flow, although the low-pressure flames could withstand inhibitor (CF<sub>3</sub>Br) levels up to 15% of total flow without being extinguished. Fuel, oxidizer, and inhibitor were mixed together prior to their entering the final mixing section immediately below the burner frit. Typically, an Ar shroud (3 L/min) was flowed around the flame to minimize absorption by cold gas in the line of sight. Gas flow was controlled by a MKS Instruments Inc. Type 147B gas flow controller. Total pressure within the burner

Received 28 May 1996; accepted 4 October 1996.

\* Author to whom correspondence should be sent.

† The project was originally funded under the auspices of the Strategic Environmental Research and Development Program (SERDP) of the U.S. Department of Defense.

chamber was maintained near 20 Torr, although stable flames could be maintained from near-atmospheric to less than 2 Torr.

Mid-infrared laser radiation used to probe the low-pressure, premixed flames was provided by a liquid nitrogen-cooled tunable diode laser (cryogenically cooled Pb-salt laser source and monochromator system from Laser Photonics, Analytics Division, Inc.) and detected by using a liquid nitrogen-cooled HgCdTe narrow-band infrared detector. Laser output is frequency modulated (1 kHz) and is collimated and mode-selected prior to its entering the low-pressure chamber. After passing through the flame region, the mid-infrared laser beam is focused onto the liquid nitrogen-cooled HgCdTe detector. Lock-in detection at the modulation frequency effectively discriminates against emission from the flame. Entrance and exit apertures mounted on the evacuable burner chamber restrict the maximum beam diameter through the flame to 1.5 mm.

FT-IR absorption measurements through low-pressure premixed flames were made by using a Mattson Sirius FT-IR spectrometer. The collimated beam from the infrared spectrometer was taken externally to the instrument, apertured to 1 mm diameter, brought to a focus above the center of the burner, and then refocused onto a liquid nitrogen-cooled HgCdTe wide-band infrared detector. FT-IR emission measurements used a Midac Model G-5001-FH spectrometer system modified in-house to measure radiation emitted from the flame. Because of the modular nature of the Midac spectrometer, modification of the instrument to measure emission spectra was straightforward, and consisted of repositioning of the interferometer "brick" and liquid nitrogen-cooled In-Sb detector to accommodate the burner flame as the source of radiation.

*Atmospheric-Pressure Counterflow Diffusion Flames.* The atmospheric-pressure counterflow diffusion burner assembly was fabricated at NIST<sup>2</sup> and consists of two opposing, wire-screen-covered gas ports (2.5 cm diameter). Gas port separation was adjustable but was typically several centimeters. Fuel (methane) is flowed into the flame region through the lower port. Oxidizer (oxygen or air) and inhibitor are flowed into the flame region through the upper port. The flame appears as a thin, flat, luminous disk (with slight edge curvature pointing up towards the exhaust shroud) located between the fuel and oxidizer ports. All gases are exhausted from the flame region through an exhaust port, which forms a shroud around the oxidizer port. Typical flow rates were 600 mL/min oxygen and 500 mL/min methane. When air was used as the oxidizer, the air flow rate was 2.2 L/min and the methane flow rate was 1.1 L/min. Inhibitor was always added on the oxidizer side only, and inhibitor flow varied up to a maximum of 1.3% of the total flow for each system investigated. These flow parameters were selected because they gave the most stable flame for that particular fuel/oxidizer combination.

Fuel and oxidizer flow was controlled by a MKS Instruments Inc. Type 147B gas flow controller. Although the burner exhaust shroud was connected to a high-volume vacuum pump, it was necessary to contain the atmospheric-pressure counterflow diffusion burner within a large box equipped with optical ports and a chimney at-

tached to a fume hood. This arrangement was made to prevent toxic gases (HF and CF<sub>2</sub>O) from entering the main laboratory.

**Real-Scale Fires.** Two types of JP-8 fuel pool fires were investigated. The first fire investigated was a JP-8 fuel pool fire burning in air. Infrared spectra of gases removed from the flame environment were measured by using a Midac Corporation Model G-5001-FH Fourier transform spectrometer system operating at 0.5-cm<sup>-1</sup> resolution. Detection of infrared radiation was by a liquid nitrogen-cooled HgCdTe detector. The interior of the spectrometer was purged with dry nitrogen, and the spectrometer system was ruggedized, by the manufacturer, for outdoor use. This ruggedization consisted of kinematic mounting of all optical components and manufacture of all transmissive optics (including the beamsplitter) from ZnSe.

Samples of gases were removed from the flame environment and flowed through a 10-m-pathlength multipass optical cell (internal volume approximately 2300 cm<sup>3</sup>) at a flow rate of 6 L/minute. The gas manifold and the 10-m-pathlength multipass optical cell contained within the instrument were maintained at 400 K to prevent condensation. The tubing leading from the stainless steel probe (0.25-in.-o.d. 304 stainless steel tubing) to the instrument gas manifold was of Teflon<sup>®</sup> and was unheated. No condensation was observed within the Teflon<sup>®</sup> tubing leading from the probe to the spectrometer, but a small amount of black soot formed on the interior surface of the Teflon<sup>®</sup> tubing during testing. It is assumed that measured concentrations of gases normally highly soluble in water (e.g., HF and CF<sub>2</sub>O) were always less than actual, because of reactions of these gases with water condensed on the walls of the probe. Fires were fueled by 3 gallons of JP-8 fuel placed in a 20-cm-deep square pan approximately 1 m on a side. The stainless steel probe, approximately 3 m in length, was located at the edge of the pan, approximately 1 m above the surface of the liquid fuel.

Prior to ignition of the fuel (accomplished with an oxygen-acetylene torch), gas flow to the multipass cell was begun, a background scan set was measured, and a series of sample scan sets was begun. Each scan set consisted of 10 coadded scans measured at 0.5-cm<sup>-1</sup> resolution. Collection of these scan sets continued throughout the course of the experiment. Three minutes after ignition of the fuel (to allow the fire to stabilize), chemical inhibitor (either CF<sub>3</sub>Br or C<sub>3</sub>F<sub>7</sub>H) was sprayed into the fire with a hand-held extinguisher. The inhibitor [CF<sub>3</sub>Br (Halon 1301, DuPont) or C<sub>3</sub>F<sub>7</sub>H (trade name FM200, Great Lakes Chemical)] was applied to the fire from the side opposite to the location of the probe, with the inhibitor stream directed toward the lower portion of the fire.

The second type of fire investigated was a JP-8 fuel pool fire burning in the crew compartment of the ballistic hull of a Bradley Fighting Vehicle. For these tests, a 0.3-m<sup>2</sup> pan was filled to a depth of approximately 1 cm with JP-8 fuel. All doors and hatches were closed, and the fire was ignited through a small access port with an oxygen-acetylene torch. After approximately 15 s, the onboard fire suppression system, consisting of a bottle filled with approximately 3 kg inhibitor and pressurized with N<sub>2</sub> to 800 psi, was deployed. Full inhibitor release and fire extinguishment (when successful) occurred in less than 1 s.

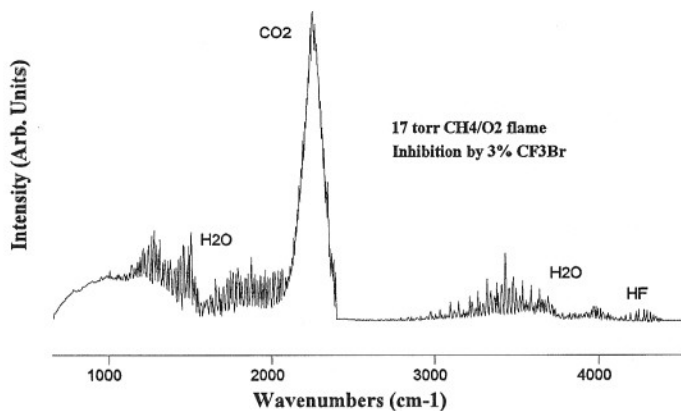


FIG. 1. The FT-IR emission spectrum of gases present 10 mm above the burner surface of a 17 Torr, stoichiometric, premixed gas,  $\text{CH}_4/\text{O}_2$  flame to which 3%  $\text{CF}_3\text{Br}$  has been added.

Placed within the crew compartment of the vehicle (see Fig. 6) was a GRIN-lens tipped fiber optic, emitting laser radiation at  $7665\text{ cm}^{-1}$ . The source of the near-infrared laser radiation was a tunable diode laser spectrometer system (thermoelectrically cooled InGaAsP distributed feedback laser source) manufactured by Southwest Sciences, Inc. The laser radiation was detected by a room-temperature InSb photodiode detector (distance from fiber-optic source = 10 cm). This frequency corresponds to the frequency of the P(2) line of the first overtone of the fundamental HF vibration. The laser was scanned at 50 Hz over the spectral region of interest (approximately  $0.05\text{ cm}^{-1}$  on either side of  $7665\text{ cm}^{-1}$ ) and frequency modulated at 50 kHz during each scan through the spectral region of interest. Detector output was demodulated at 100 kHz (SRS Inc. Model 850 lock-in amplifier), and digitized with the use of an oscilloscope (Lecroy 9360). Data collection was initiated prior to ignition of the fire. Each data point (Figs. 7 and 8) corresponds to one scan over the spectral region near  $7665\text{ cm}^{-1}$ , at a time resolution of 20 ms. A new data point was measured every 2 s, for the duration of the experiment.

## RESULTS

**Laboratory-Scale Fires.** *Fourier Transform Spectroscopy.* Initial measurements in our laboratory<sup>2</sup> using FT-IR spectroscopy to investigate low-pressure (20 Torr) premixed  $\text{CH}_4/\text{O}_2$  flames inhibited by up to 15%  $\text{CF}_3\text{Br}$  showed no evidence of  $\text{CF}_2\text{O}$  formation, even though calculations indicated<sup>4</sup> that  $\text{CF}_2\text{O}$  should be formed in small amounts. As an example, Fig. 1 is an FT-IR emission spectrum of gases present 10 mm above the burner surface (spatial resolution approximately 1 mm) of a 17 Torr premixed  $\text{CH}_4/\text{O}_2$  flame to which 3%  $\text{CF}_3\text{Br}$  has been added. This spectrum is similar in appearance to an absorbance spectrum measured through the flame at a similar height above the burner surface.<sup>3</sup> Emission spectroscopy was used because experiments using absorption spectroscopy to measure combustion products in flames are often complicated by absorption of radiation by cold gas species outside of the flame zone. Although significant amounts of HF are detected near  $4000\text{ cm}^{-1}$ , there is no evidence of  $\text{CF}_2\text{O}$  gas (strongest feature near  $1900\text{ cm}^{-1}$ ) at any height within the flame.

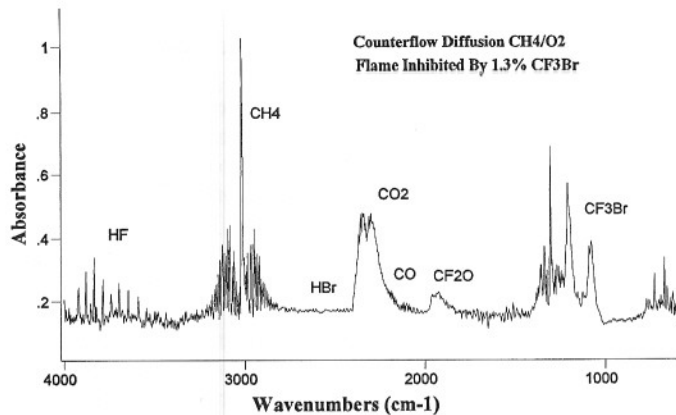


FIG. 2. The FT-IR absorbance spectrum measured through an atmospheric-pressure counterflow diffusion  $\text{CH}_4/\text{air}$  flame inhibited by 1.3%  $\text{CF}_3\text{Br}$ .

Figure 2 shows the FT-IR absorption spectrum measured through an atmospheric-pressure counterflow diffusion  $\text{CH}_4/\text{air}$  flame<sup>3</sup> inhibited by 1.3%  $\text{CF}_3\text{Br}$ . In this spectrum, formation of  $\text{CF}_2\text{O}$  gas is measured near  $1900\text{ cm}^{-1}$ , as well as CO ( $2100\text{ cm}^{-1}$ ), HBr ( $2700\text{ cm}^{-1}$ ), and HF ( $4000\text{ cm}^{-1}$ ). More species are observed in the atmospheric-pressure counterflow diffusion flame than in the low-pressure premixed flame, because the peak temperature in the counterflow diffusion  $\text{CH}_4/\text{air}$  flame is several hundred Kelvins lower<sup>3</sup> than in the low-pressure  $\text{CH}_4/\text{O}_2$  flame. Species generated in the lower-temperature flame have a longer residence time than do those in the low-pressure  $\text{CH}_4/\text{O}_2$  flame, allowing measurement of  $\text{CF}_2\text{O}$  and HBr in the counterflow diffusion  $\text{CH}_4/\text{air}$  flame.

These initial studies using FT-IR spectroscopy provide spectroscopic evidence that gas production during Halon inhibition of fires is highly dependent on the fire type and conditions. In our investigations aimed at validating flame modeling calculations,<sup>5</sup> we use low-pressure flames because, at low pressure, flame zones are expanded, and more information is available from optical measurements with the use of our finite spatial resolution (typically 1 mm). However, for measurements of some species present at low concentrations within the low-pressure flame, we are limited by the optical resolution of most commercial FT-IR spectrometers (usually on the order of  $0.5\text{ cm}^{-1}$ ).

*Tunable Diode Laser Spectroscopy.* To measure species at concentrations below the detection limit of our Fourier transform spectrometer, we employ tunable diode laser absorption spectroscopy using phase-sensitive detection. The instrumental methods employed in using such derivative-based spectroscopies have been well characterized in the literature.<sup>6</sup> The principal advantages of the technique are high resolution (typically better than  $0.0005\text{ cm}^{-1}$ ); increased sensitivity, because of the use of phase-sensitive detection; and, at high laser modulation frequencies, low source noise.

Figure 3 shows second-derivative mid-infrared tunable diode laser absorption spectra measured through rich and lean 21 Torr  $\text{CH}_4/\text{O}_2/\text{Ar}$  flames doped with 5%  $\text{CF}_3\text{Br}$ . These spectra were measured by using a probe beam waist of 1.5 mm, with the beam center axis 3 mm above

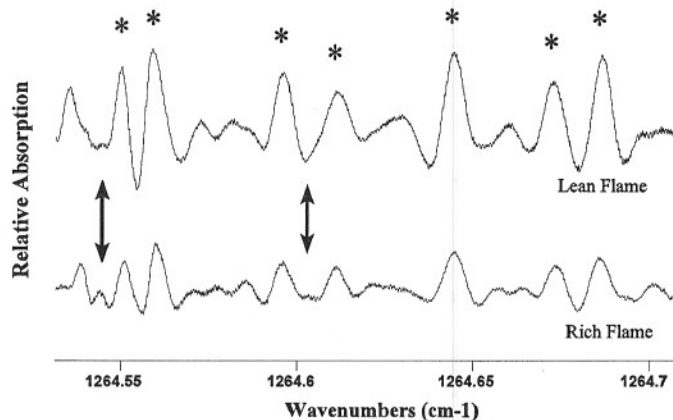


FIG. 3. Second-derivative mid-infrared tunable diode laser absorption spectra measured through rich and lean 21 Torr premixed  $\text{CH}_4/\text{O}_2$  flames inhibited by 5%  $\text{CF}_3\text{Br}$ . Spectra for each flame were measured 3 mm above the burner surface. The asterisks indicate the position of an absorption feature due to  $\text{CF}_2\text{O}$ . Double-headed arrows indicate positions of  $\text{CF}_3$  absorption. Note that  $\text{CF}_2\text{O}$  absorption is greater in the lean flame, while  $\text{CF}_3$  absorption is greater in the rich flame (see text).

the burner surface. The spectral region of interest was determined by the reported frequencies of  $\text{CF}_3$  and  $\text{CF}_2\text{O}$  absorptions,<sup>7</sup> by the spectral structure of the reference gas ( $\text{N}_2\text{O}$ ), and by the output range of our diode laser system. The spectral region selected was from 1264.3 to 1264.7  $\text{cm}^{-1}$ . In addition to encompassing several absorption lines of  $\text{CF}_3$  and  $\text{CF}_2\text{O}$ , this spectral region was selected because it was free from absorptions from the reference gas ( $\text{N}_2\text{O}$ ), as well as  $\text{CH}_4$ ,  $\text{CF}_3\text{Br}$ ,  $\text{CO}_2$ , and  $\text{H}_2\text{O}$ , and because the  $\text{CF}_2\text{O}$  absorption features present in this region, although dense, were recognizable, and they had a weak temperature dependence as calculated with the use of the HITRAN<sup>8</sup> database. Because of the low anticipated concentrations of the  $\text{CF}_3$  radical, we did not consider interferences from  $\text{C}_2\text{F}_6$ , although for higher concentrations of the  $\text{CF}_3$  radical it has been shown that absorption from  $\text{C}_2\text{F}_6$  may be important.<sup>7</sup> The  $\text{CF}_2$  radical has no reported absorbance in this region.<sup>9</sup> The main experimental difficulty in detecting  $\text{CF}_3$  in flames inhibited by Halons is that the spectral features from the radical are usually obliterated by the dense spectral structure of  $\text{CF}_2\text{O}$ .

Several features may be noted from the spectra shown in Fig. 3. Most importantly, features due to absorption of radiation by  $\text{CF}_2\text{O}$  (marked with an asterisk) are seen to be more intense for the lean flame (1.9 L/m  $\text{O}_2$ , 0.76 L/m  $\text{CH}_4$ , 1.0 L/m Ar) than for the rich flame (1.7 L/m  $\text{O}_2$ , 1.0 L/m  $\text{CH}_4$ , 1.0 L/m Ar). This is because excess oxygen in the lean flame may compete with the H atom for reactions with the  $\text{CF}_3$  radical and  $\text{CF}_2$  radical, increasing  $\text{CF}_2\text{O}$  formation relative to that occurring in a rich (oxygen-poor) flame.<sup>10</sup> We have found that comparing rich- and lean-flame infrared spectra of flames with similar levels of fluorocarbon inhibitor is a useful way of aiding the identification of lines arising from absorption of infrared radiation by  $\text{CF}_2\text{O}$ . This observation reflects the different way the inhibitor participates in rich and lean combustion environments and may provide insight into controlling amounts of HF and  $\text{CF}_2\text{O}$  in combustion gases.

Figure 4 shows measurements of second-derivative spectra, over the same spectral region shown in Fig. 3,

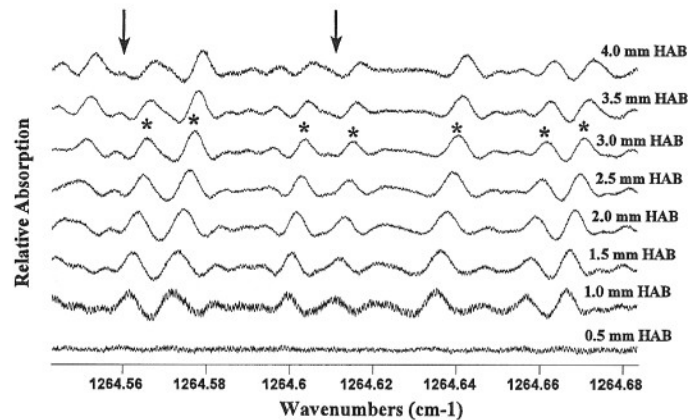


FIG. 4. Second-derivative mid-infrared tunable diode laser absorption spectra measured through a premixed, rich,  $\text{CH}_4/\text{O}_2/\text{Ar}$  flame to which 5%  $\text{CF}_3\text{Br}$  has been added, measured as a function of laser beam height above burner (HAB) surface. The asterisks indicate the position of an absorption feature due to  $\text{CF}_2\text{O}$ . Arrows indicate positions of  $\text{CF}_3$  absorption. Note how  $\text{CF}_3$  absorption first increases, then decreases, with increasing height above burner surface, in agreement with flame modeling calculations.

through the rich, 21 Torr, premixed  $\text{CH}_4/\text{O}_2/\text{Ar}$  flame doped with 5%  $\text{CF}_3\text{Br}$  (and shown in Fig. 3), as a function of height above the burner surface. As in Fig. 3, absorption by  $\text{CF}_2\text{O}$  is indicated by asterisks. Arrows indicate the position of absorption of infrared radiation by  $\text{CF}_3$ . For Fig. 4, two features, at 1264.557 and 1264.604  $\text{cm}^{-1}$ , corresponding to absorption by  $\text{CF}_3$ , are not obscured by absorption by  $\text{CF}_2\text{O}$ . The absorption at 1264.557  $\text{cm}^{-1}$  is more intense than the absorption at 1264.604  $\text{cm}^{-1}$ , and first appears at 1 mm above the burner surface. The absorption at 1264.557  $\text{cm}^{-1}$  disappears as height above the burner surface is increased. The smaller absorption near 1264.604  $\text{cm}^{-1}$  appears approximately 3 mm above the burner surface, and vanishes at approximately 4 mm above the burner surface.

We believe the absorption features seen in the spectra of Halon 1301-inhibited flames at 1264.557 and 1264.607  $\text{cm}^{-1}$  are the first optical measurement of the  $\text{CF}_3$  radical in Halon-inhibited low-pressure flames. The successive spectra show an increase, followed by a decline, with height above the burner surface, for the two features at frequencies previously assigned to the  $\text{CF}_3$  radical. This spatial dependence is consistent with predictions from flame model calculations of fluorine-inhibited flames.<sup>10</sup> The intensity of these two features, in proportion to  $\text{CF}_2\text{O}$  absorption, changes in qualitative agreement with flame modeling calculations. However, it may be seen from Fig. 4 that there remain many unassigned features in each spectrum, so an unambiguous assignment of these weak features to  $\text{CF}_3$  cannot be made until more than two transitions have been identified.

**Real-Scale Fires. Fourier Transform Spectroscopy.** Measurement of gases produced during real-scale fire testing was performed at the Aberdeen Test Center. All fires investigated used JP-8 as fuel. JP-8 is a turbine engine fuel composed of long-chain ( $\text{C}_n$ ,  $n > 5$ ) hydrocarbons. Figure 5 shows the FT-IR absorbance spectrum of gases removed from the vicinity of the fire during inhibition of the fire by Halon 1301 ( $\text{CF}_3\text{Br}$ ). Evident from this spectrum are features due to HF, HCl, HBr, CO, and

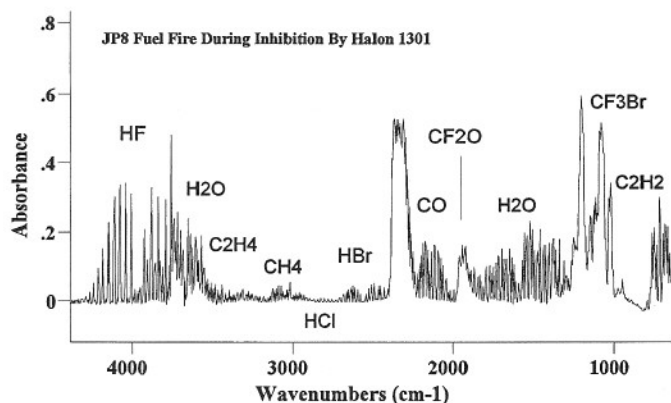


FIG. 5. The FT-IR absorbance spectrum of gas removed from the vicinity of a JP-8 fuel pool fire during inhibition by  $\text{CF}_3\text{Br}$  (Halon 1301).

$\text{CF}_2\text{O}$ , as well as other species participating in the combustion. Most noticeable is the difference between species present in this fire vs. those observed in the laboratory-scale fires. Most significant are the prominent features due to  $\text{HBr}$  and  $\text{CF}_2\text{O}$ . We believe the  $\text{HCl}$  present in the flame arises from chlorine impurities in the  $\text{CF}_3\text{Br}$ , although no effort was made on our part to verify impurities present in any of the inhibitors used in these experiments. The optically determined concentrations of gases present during inhibition of open-air JP-8 pan fires by  $\text{CF}_3\text{Br}$  (Halon 1301) and  $\text{C}_3\text{F}_7\text{H}$  (FM-200) have recently been reported by us elsewhere.<sup>3</sup>

**Tunable Diode Laser Spectroscopy.** Results from measurements using Fourier transform spectroscopy (Fig. 5) showed significant lethal concentrations of  $\text{HF}$  and  $\text{CF}_2\text{O}$  gas produced during inhibition of open-air JP-8 fuel pan fires by  $\text{CF}_3\text{Br}$ . For testing of fire inhibition by Halons in occupied areas, it is important to measure *in situ* the time evolution of any toxic gases produced during the inhibition event. This is important for measurement of  $\text{HF}$ , since we have observed that  $\text{HF}$  reacts rapidly with most surfaces, especially in the presence of moisture. For this reason, tunable diode laser spectroscopy was chosen to be one of the diagnostics employed during testing.  $\text{HF}$  was selected as the most important gas to monitor, since  $\text{HF}$  typically has the highest partial pressure of any of the Halon-inhibited flame toxic gas products.

Figure 6 shows a schematic diagram of the facility for measuring gases produced during suppression of JP-8

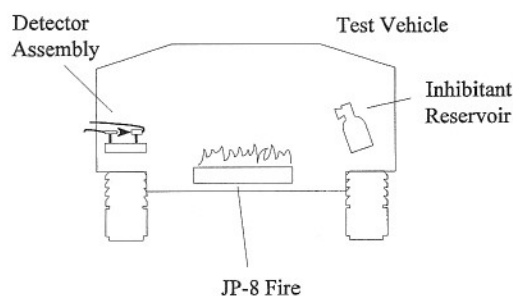


FIG. 6. A schematic diagram of the test facility for measuring gases produced during suppression of JP-8 fuel pool fires occurring within crew compartments of Army vehicles. The detector assembly consists of an extractive FT-IR probe and an *in situ* NIR diode laser emitter-detector assembly.

HF Production - Crew Compartment

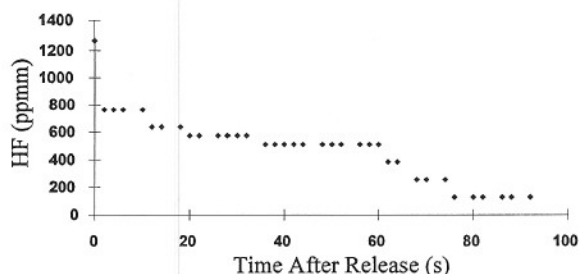


FIG. 7. A graph of  $\text{HF}$  production (ppmm) vs. time after release of  $\text{C}_3\text{F}_7\text{H}$  inhibitor (FM-200) for a JP-8 fuel pool fire occurring within the crew compartment of an Army combat vehicle. For this test, the inhibitor extinguished the fire.

fires occurring within the crew compartment of a ballistic hull and turret of an Army combat vehicle. The  $\text{HF}$  diagnostic uses a near-infrared tunable diode laser operating at  $7665\text{ cm}^{-1}$ . This frequency corresponds to the frequency of the P(2) line of the first overtone of the fundamental  $\text{HF}$  vibration. There are several reasons to use diode lasers operating in the near-infrared. For  $\text{HF}$  diagnostics, however, the most important is that mid-infrared diode lasers operating at the fundamental frequency (near  $4000\text{ cm}^{-1}$ ) are not yet available. Other reasons for using a near-infrared tunable diode laser-based diagnostic include the ease of transmission of the laser radiation through optical fibers, the operation at temperatures attainable with thermoelectric coolers ( $\sim 270\text{ K}$ ), the low cost of detectors, and the ability to significantly reduce laser output noise through the use of kHz modulation techniques.<sup>11</sup>

Figure 7 is a graph of  $\text{HF}$  gas production (in ppmm, parts per million meter), measured with the use of the near-infrared tunable diode laser, vs. time immediately after release of  $3.4\text{ kg}$  of  $\text{C}_3\text{F}_7\text{H}$  (FM-200) into a JP-8 fuel pan fire (area  $\sim 0.3\text{ m}^2$ ) burning within the closed crew compartment of the ballistic hull and turret of a Bradley Fighting Vehicle. The Halon was dispersed into the fire in approximately 1 s. Fire extinguishment occurred during dispersal of the inhibitor. Figure 8 is a graph of  $\text{HF}$  gas production (in pptm, parts per thousand

HF Production - Crew Compartment

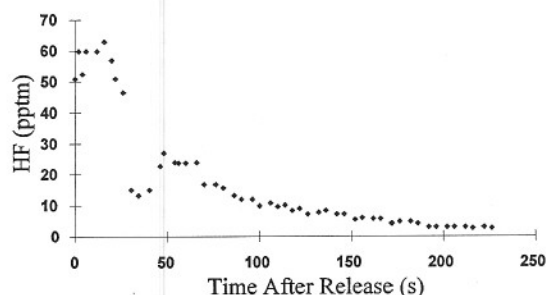


FIG. 8. A graph of  $\text{HF}$  gas production (pptm) vs. time immediately after release of  $\text{C}_3\text{F}_7\text{H}$  (FM-200) into a JP-8 fuel pool fire burning within the closed crew compartment of an Army combat vehicle. Unlike the data shown in Fig. 7, for this test the fire was not extinguished by the inhibitor. The dip in  $\text{HF}$  concentration near 40 s is due to activation of the back-up  $\text{CO}_2$  extinguisher system.

meter), measured with the use of the near-infrared tunable diode laser, vs. time for an identical test, except that the fire was not extinguished by the Halon. The only difference between tests is a slight change in position of the nozzle of the cannister from which the Halon is dispersed. From Figs. 7 and 8, it may be seen that peak HF production in the fire not extinguished by the Halon is approximately 50 times higher than in the fire in which extinguishment by the Halon occurred immediately. The dip in HF concentration in Fig. 8 near 40 s marks the time at which the back-up CO<sub>2</sub> extinguishment system was used to put out the fire. These results indicate that time to suppression, when Halon-based fire inhibitants are used, is a critical factor in determining the amount of toxic gas (HF) produced during fire fighting. We believe these results are the first real-time, quantitative, *in situ* measurements of HF production during inhibition of real-scale fires using Halons.

## CONCLUSION

Optically based measurements can provide valuable diagnostic information necessary for determination and analysis of mechanisms and efficiencies of Halon fire inhibitants. We have shown that production of toxic gases associated with fire inhibition by Halons, particularly HF and CF<sub>2</sub>O, is dependent on the type and conditions of the fire being investigated. We have measured differences in concentrations of CF<sub>3</sub> produced in rich and lean flames inhibited by CF<sub>3</sub>Br. Finally, we have shown that the time evolution of HF gas produced during inhibition is dependent on whether fire suppression is accomplished immediately after application of Halon inhibitant. We are currently exploring the application of the diagnostic techniques mentioned in this report to more types of fires and extending the methods described here to even more extreme environmental conditions.

## ACKNOWLEDGMENTS

We would like to acknowledge support from Mr. Steve McCormick at TACOM and also from the SERDP program of the DoD. We also wish to acknowledge the support of Craig Herud, Bill Bolt, and Stan Polyanski of the Aberdeen Test Center (ATC), who were responsible for overseeing the running of the tests and of the testing facility, and without whom these tests would have been impossible.

1. K. L. McNesby, R. G. Daniel, and A. W. Miziolek, *Appl. Opt.* **34**, 3318 (1995).
2. K. L. McNesby, R. G. Daniel, J. M. Widder, and A. W. Miziolek, *Appl. Spectrosc.* **50**, 126 (1996).
3. S. H. Modiano, K. L. McNesby, P. E. Marsh, W. Bolt, and C. Herud, *Appl. Opt.* **35**, 4004 (1996).
4. A. W. Miziolek, A. E. Finnerty, R. G. Daniel, K. L. McNesby, W. Tsang, V. I. Babushok, M. R. Zachariah, P. R. Westmoreland, and D. R. F. Burgess, Jr., "Fundamental Studies of Fire Extinguishment for Predicting Halon Alternative Compound Behaviour", in *Proceedings of the 1994 Army Science Conference*, Orlando, Florida (1994).
5. R. G. Daniel, K. L. McNesby, and A. W. Miziolek, *Appl. Opt.* **35**, 4018 (1996).
6. P. L. Varghese and R. K. Hanson, *J. Quant. Spectr. Rad. Transfer* **24**, 279 (1980).
7. C. Yamada and E. Hirota, *J. Phys. Chem.* **78**, 1703 (1983).
8. L. S. Rothman, R. R. Gamache, R. H. Tipping, C. P. Rinsland, M. A. H. Smith, D. C. Brenner, V. Malathy Devi, J.-M. Flaud, C. Camy-Peyert, A. Perrin, A. Goldman, S. T. Massie, L. R. Brown, and R. A. Toth, *J. Quant. Spectrosc. Radiat. Transfer* **48**, 469 (1992) (1992 HITRAN database).
9. P. B. Davies, W. Lewis-Bevan, and D. K. Russell, *J. Chem. Phys.* **75**, 5602 (1981).
10. V. Babushok, D. F. R. Burgess, Jr., G. Linteris, W. Tsang, and A. W. Miziolek, "Modeling of Hydrogen Fluoride Formation From Flame Suppressants During Combustion", in *Proceedings of the 1995 Halon Options Technical Working Conference* (New Mexico Engineering Research Institute, Albuquerque, 1995), pp. 239-250.
11. D. S. Bomse, D. C. Houde, D. B. Oh, J. A. Silver, and A. C. Stanton, "Diode Laser Spectroscopy for On-Line Chemical Analysis", in *Optically Based Methods For Process Analysis*, SPIE Vol. 1681 (SPIE, Bellingham, Washington, 1992), p. 138.